Eur Radiol (2004) 14:1498–1507
DOI 10.1007/s00330-004-2265-9

Olivier Clément
Alain Luciani

Imaging the lymphatic system: possibilities and clinical applications

Received: 23 July 2003
Revised: 22 September 2003
Accepted: 5 January 2004
Published online: 9 March 2004

O. Clément (✉)
Service de Radiologie,
Hôpital Européen Georges Pompidou,
20 rue Leblanc, 75908 Paris Cedex 15,
France
e-mail: clement@necker.fr
Tel.: +33-1-56093851
Fax: +33-1-56093850

A. Luciani
Service de Radiologie,
Hôpital Henri Mondor,
Créteil, France

Abstract The lymphatic system is anatomically complex and difficult to image. Lymph ducts are responsible for the drainage of part of the body's interstitial fluid. Lymph nodes account for the enrichment of lymph fluid, and can be involved in a large variety of diseases, especially cancer. For a long time, lymphatic imaging was limited to the sole use of conventional lymphography involving invasive procedures and patient discomfort. New contrast agents and techniques in ultrasound, nuclear medicine, and MR imaging are now available for imaging of both the lymphatic vessels and the lymph nodes. The objective of this review is to discuss the different imaging modalities of the lymphatic system, with a special focus on the new possibilities of lymphatic imaging including enhanced MR lymphography, sentinel node and positron emission tomography imaging, and contrast-enhanced ultrasound.

Keywords Lymphatic system · Magnetic resonance (MR) · Contrast enhancement · Computed tomography (CT) · Lymph node

Introduction

The lymphatic system is complex and its imaging remains challenging. First, the lymphatic system is not an organ, but rather links different structures together, from small lymphatic capillaries back to main ducts, through lymph nodes and valves. Each of these structures can be imaged independently from one another. Second, the lymphatic system can be involved in a wide variety of pathologies including neoplastic and infectious diseases. Furthermore, congenital or acquired impairments can lead to lymph flow disturbances, where clinical examination usually does not provide sufficient information to allow a precise diagnosis. Owing to the development of new contrast agents and imaging techniques such as MR lymphography, contrast-enhanced ultrasound, and positron emission tomography (PET) imaging, the field of lymphatic imaging is growing rapidly.

After briefly reviewing the lymphatic anatomy and physiology, we detail the means of contrast agent administration in the lymphatic system and focus on the role of MR lymphography, sentinel node imaging, PET imaging, and ultrasound in the assessment of lymphatic vessels and lymph nodes.

Lymphatic anatomy and physiology

The lymphatic system drains part of the interstitial fluid from small capillaries to lymphatic vessels through lymph nodes, and finally to the venous system via a common jugular anastomosis.

Lymph vessels

Although deriving from perivenous mesenchymal clefts at the end of the fifth gestation week, the lymphatic system is independent of the venous system. Six distinct lymphatic territories represented by saccular lymphatic dilatations can be individualized during the initial stages of lymphatic development including two jugular, two il-

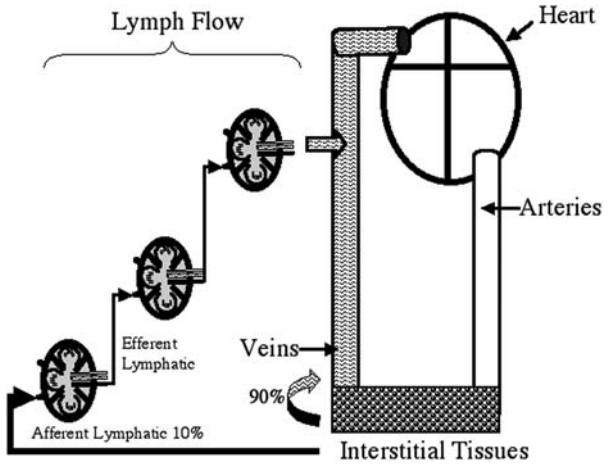

Fig. 1 Schematic representation of the lymphatic system. Lymph ducts allow the drainage of close to 10% of the interstitial fluid, while the remaining 90% is taken up directly by the venous system. In the lymphatic system, the interstitial fluid continuously circulates along the lymphatic vessels passing through a series of holding points represented by lymph nodes

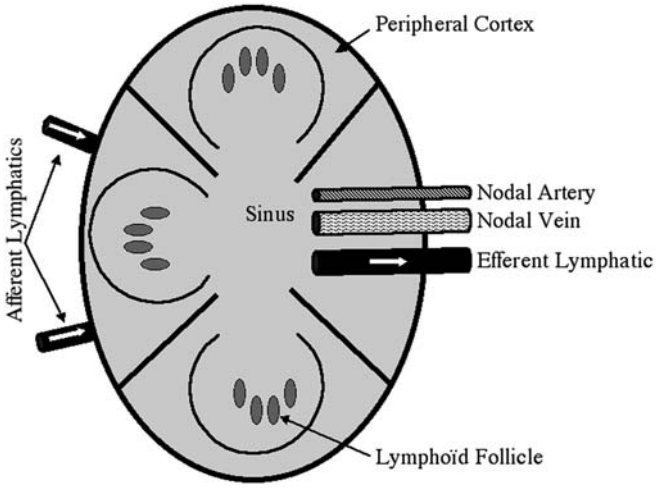

Fig. 2 Schematic representation of a lymph node. Lymph nodes separate afferent from efferent lymphatic vessels. Moreover, all lymph nodes receive specific blood supply through dedicated arteries and veins converging toward the node sinus

iac, one retroperitoneal, and the cysterna chyli territories. These six territories eventually communicate through lymphatic vessels, converging toward the cysterna chyli located between the T11 and L2 levels. Above the diaphragm, lymph vessels represented by the thoracic ducts usually merge and drain into the venous angle between the internal left jugular vein and the left subclavian vein. A general schematic representation of the lymphatic system is shown in Fig. 1. Anatomical variations of major lymphatic trunks are frequent including plexiform dilatations, duplications, or congenital absences.

Lymphatic capillaries allow the drainage of close to 10% of all interstitial fluid, while the remaining 90% is taken up by the venous system. The interstitial fluid continuously circulates along the lymphatic vessels passing through a series of holding points (lymphatic valves and lymph nodes; Fig. 1).

When lymphatic circulation is impaired, interstitial fluid accumulates in the extremities. The congenital or acquired defects of lymphatic vessels are, respectively, responsible for primary (within the first 5 years of life) or secondary lymph flow disorders [1].

The composition of lymph differs from that of plasma with a higher percentage of lipids (chylomicrons), particularly in the thoracic duct and a lower percentage of proteins [2] (Table 1). As a result, obstruction of the thoracic duct, whether because of trauma or because of mediastinal invasion, results in chylous lymph accumulation in the thorax better known as chylothorax [3]. Moreover, the lymphatic circulation favors the exchanges between the lymph itself and the reticuloendothelial system. This role is mainly delegated to the lymph nodes.

Table 1 Comparison of the metabolic components of the thoracic lymph and plasma

Component	Plasma (mean)	Thoracic duct (mean)
Proteins (g/dl)	7.1	2–4.9
Glucose (g/l)	0.7–1	0.7–1.3
Lymphocytes (Nb/mm3)	2,000	2,000–20,000

Lymph nodes

The anatomy and functional role of lymph nodes are illustrated in Fig. 2. Lymph nodes separate afferent lymphatic vessels converging toward the outer cortical surface of lymph nodes from efferent lymphatic vessels, leaving the lymph nodes from the centrally located medullary sinuses. Moreover, nodes receive specific blood supply through dedicated arteriolocapillarovenous branches (Fig. 2). As such, interstitial fluid can enter lymph nodes via either lymphatic or arteriolovenous routes. Thus, different pathways of contrast agent administration can be used and will result in different types of uptake and distribution to lymph nodes.

Means of contrast agent administration in the lymphatic system

As mentioned, three pathways of contrast injection can be distinguished: endolymphatic (direct route), interstitial (indirect route), or intravenous.

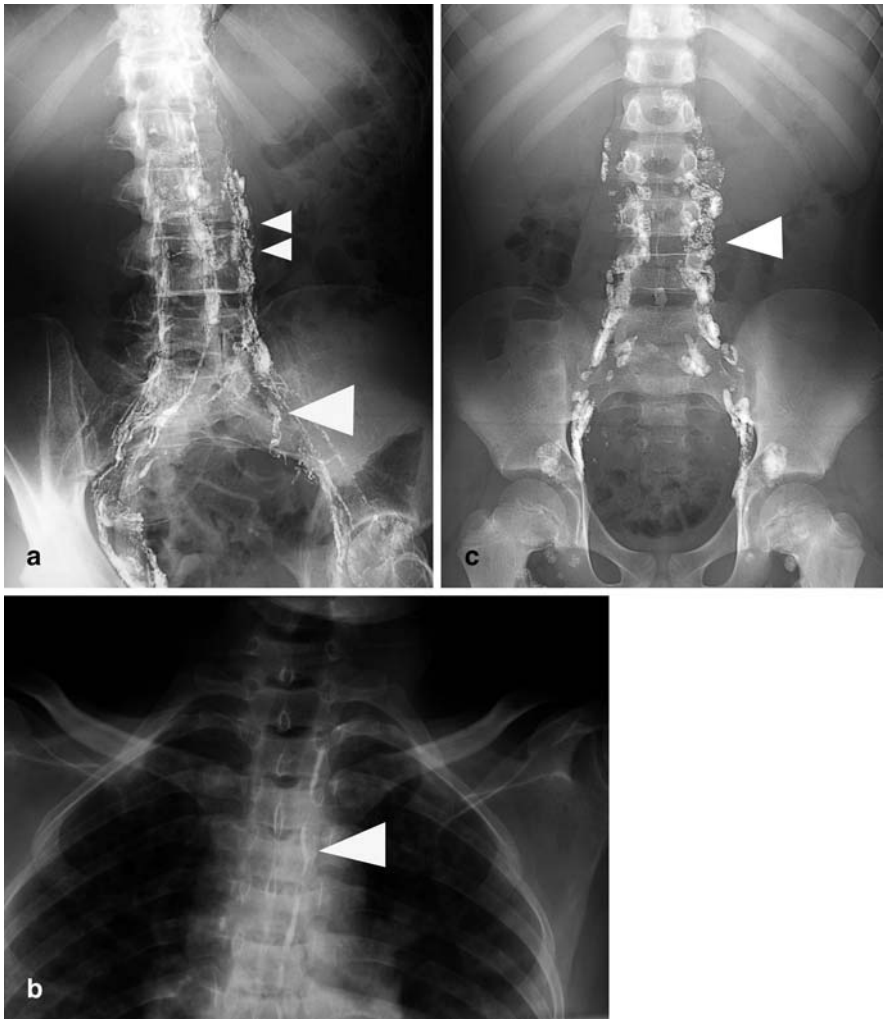

Fig. 3a–c Conventional lymphangiogram obtained from a 27-year-old patient with non-Hodgkin lymphoma. One day after direct bilateral lymphatic contrast injection into the podal extremities, both the lymphatic vessels (*arrowhead*) and the lymph nodes (*double arrowheads*) are opacified **a**. The thoracic duct (*arrowhead*) is also identified coursing to the anterior and left of the thoracic spine before its junction with the left jugular vein **b**. Two days after contrast injection only a homogeneous node enhancement persists **c**

Direct endolymphatic contrast injection route

Rationale. Injecting a contrast agent directly into distally located lymphatic vessels results in a direct opacification of the up-flowing lymph.

Technique. This well-known technique requires the catheterization of distally located lymphatics of the extremities after a small surgical incision followed by the manual injection of an oil-based contrast medium. Twenty-four hours after injection, lymph ducts are usually well depicted (Fig. 3a,b) while lymph nodes can be analyzed 48 h after injection (Fig. 3c).

Indirect interstitial contrast injection route

Rationale. Contrast agents administered intradermally enter the lymphatic vessels through the highly permeable endothelial lining of distally located fenestrated lymphatic capillaries [4].

Technique. In lymphangioscintigraphy, a small amount of radioactive tracer (500 μCi of Tc-99m albumin) is injected intradermally at a distal extremity [5] and then followed up using an appropriate Gamma camera at specific time points [6].

Indirect intravascular contrast injection route

Rationale. Intravenously administered contrast agents derived from iron particles tend to accumulate in organs belonging to the reticuloendothelial system owing to their capture by mononuclear phagocytic cells [7]. Ultrasmall iron oxide particles (USPIO) seem to be taken up more easily by the lymphatic nodes, and thus avoid massive liver and spleen capture [8]. As a result, it is believed that a single intravenous injection of such contrast agents can allow the indirect imaging of the lymphatic system.

Table 2 Different imaging techniques for imaging of lymph nodes or lymph vessels

Region	Technique				
	Conventional radiology (CR)	Computed tomography (CT)	Magnetic resonance imaging (MRI)	Ultrasound (US)	Nuclear medicine
Lymphatic vessels	Conventional lymphography	Indirect interstitial CT lymphography	Indirect interstitial MR lymphography		Lymphoscintigraphy
Lymph nodes	Conventional lymphography	Unenhanced CT (high-resolution)	Unenhanced MR (high-resolution)	High-resolution US	Lymphoscintigraphy
		Indirect interstitial CT lymphography	Indirect interstitial MRI	Color Doppler US	Positron emission tomography (PET)
			USPIO-enhanced MR lymphography	Contrast-enhanced US	

Technique. Dextran-coated USPIO contrast agents can be used in lymphatic imaging [9, 10]. Ferumoxtran (AMI 227, Sinerem-Combidex, Guerbet, France) is selectively taken up by macrophages or mononuclear cells of the reticuloendothelial system [8, 11] but its prolonged blood half-life favors its specific uptake by the lymph nodes. Two mechanisms of USPIO uptake into lymph nodes have been reported: (a) direct transcapillary passage through interendothelial junctions into medullary sinuses within lymph nodes [12, 13] and (b) capillary extravasation into the interstitium with subsequent uptake by draining lymph vessels [11]. The smaller mean diameter of USPIO particles (close to 35 nm [10]) together with their prolonged plasma half-life as opposed to that of superparamagnetic iron oxides (SPIO) could favor their transcapillary transport toward the interstitium [14]. The maximum concentration of USPIO particles in main lymphatic ducts is encountered close to 90 min following intravenous injection in rats [12]. Maximum nodal enhancement is not demonstrated prior to 12 h following contrast injection. Furthermore, USPIO particles preferentially enter lymph nodes via afferent lymph vessels, which explains why these particles are more often located at the periphery of the nodes [15]. Additionally, intravenous injection of USPIO can result in heterogeneous enhancement of lymph nodes across different lymphatic territories resulting in preferential enhancement of immunologically stimulated regions such as the celiac nodes for example [13].

Unenhanced MR imaging of the lymphatic vessels

Unenhanced imaging of the lymphatic vessels has only been recently reported owing to the development of new MR techniques. Hayashi et al. related their initial experience of nonenhanced MR lymphography in six healthy volunteers using a conventional 1.5-T device with coronal 3D half-Fourier fast spin-echo T2-weighted sequences (36 partitions/1.4 mm section thickness) [16]. The main thoracic duct was systematically identified. However, subdiaphragmatic lymphatic structures could not be imaged simultaneously owing to a limited field of view, and the impact of this technique in patients remains unknown.

Imaging the lymphatic system

Imaging lymphatic vessels

Physical examination usually provides insufficient information to clinicians regarding the lymphatic circulation. In the past, direct lymphography and indirect lymphangioscintigraphy were the only relevant examinations for the depiction of lymphatic disorders. We now focus on new imaging techniques allowing an improved depiction of lymph vessels and especially on indirect interstitial MR lymphography (Table 2).

Indirect MR lymphography for imaging of the lymphatic vessels

In analogy to indirect lymphoscintigraphy, gadolinium-based contrast agents can be injected intradermally or subcutaneously. Such T1-type of contrast agents ensure a positive lymph node enhancement on T1-weighted images [17]. Some authors have suggested using a lipophilic perfluorinated gadolinium chelate not larger than 4 nm [18]. Within 10 min of subcutaneous injection of this agent into the hind legs of pigs, subdiaphragmatic lymph nodes showed T1 enhancement. Furthermore, the thoracic duct was identified in four out of six animals. Similar results have been reported following the interstitial injection of polymeric gadolinium chelates such as Gadomer 17 (Schering AG, Berlin, Germany). This intermediate-molecular-weight (17 kDa) contrast agent allowed the enhancement of regional nodes within 15 min of injection into the hind legs of 15 dogs [19]. However, such contrast agents are still under development with no clear and present human applications. More recently, the per-

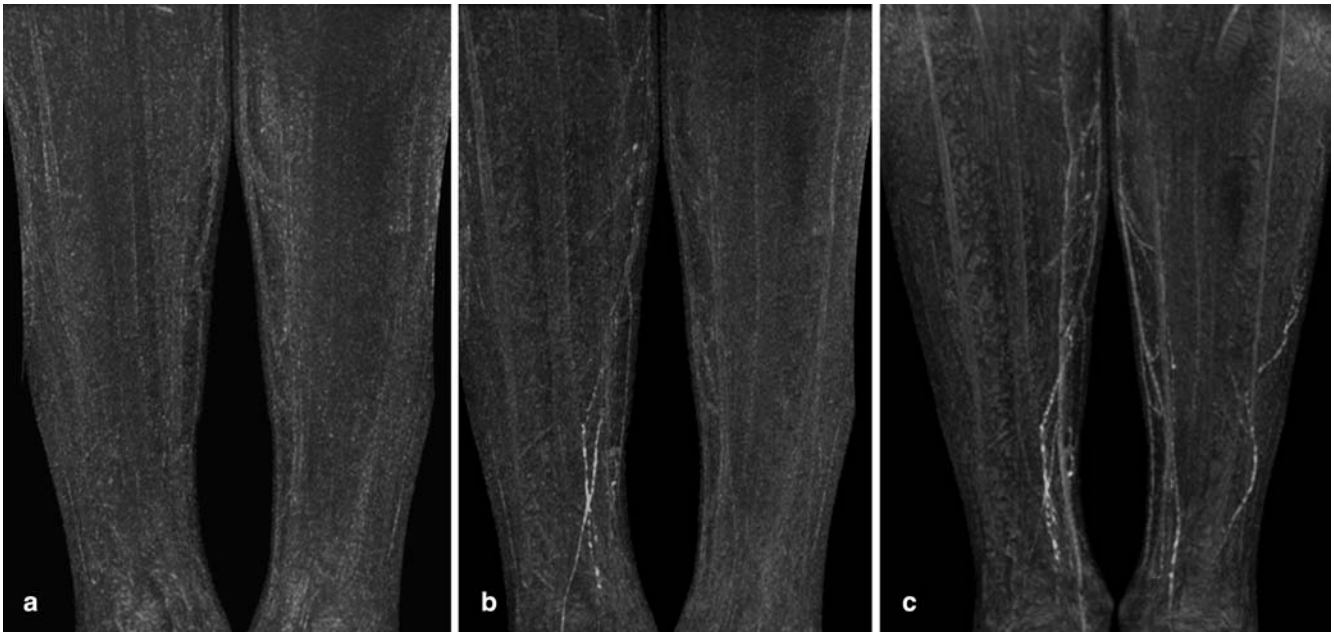

Fig. 4a–c Three-dimensional MR lymphography of the left lower limb performed before **a**, 15 min (see Fig. 5b), and 45 min **c** after the subcutaneous injection of 4.5 ml of Gd-DOTA (Dotarem) mixed with 0.5 ml of xylocaïne in the left extremity of a healthy volunteer showing the progressive opacification of distally located lymphatic vessels of the homolateral leg. (Kindly provided by Dr. Ruehm)

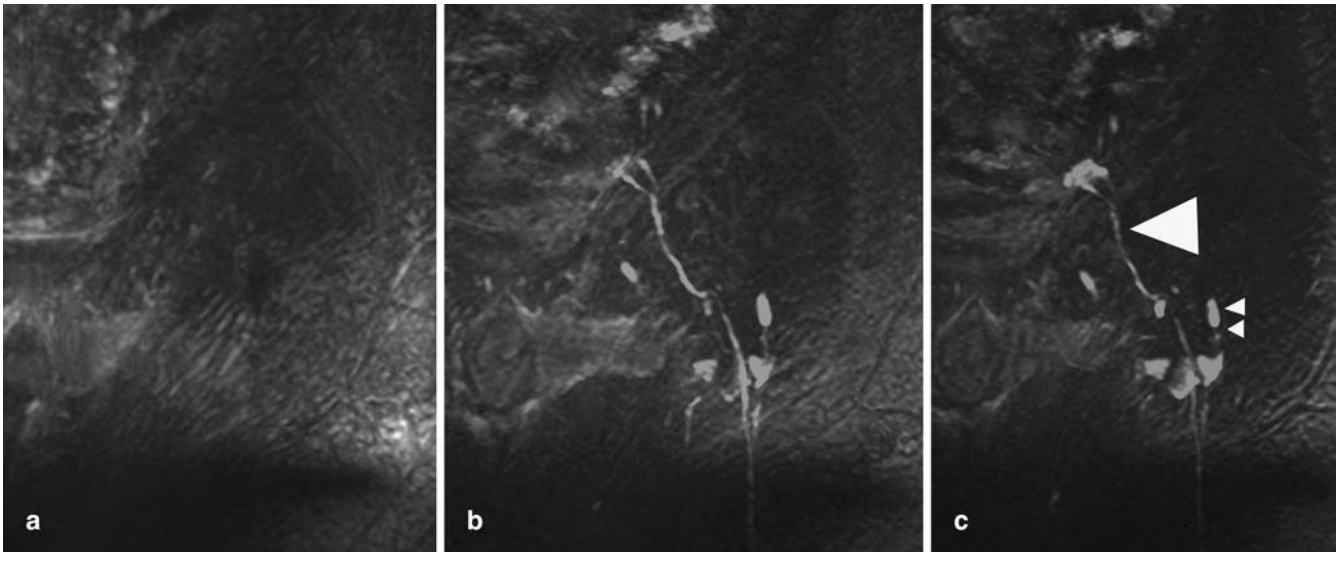

Fig. 5a–c Three-dimensional MR lymphography of the left inguinal region performed before **a**, 20 min **b**, and 50 min **c** after the subcutaneous injection of 4.5 ml of Gd-DOTA (Dotarem) mixed with 0.5 ml of xylocaïne in the left extremity of a healthy volunteer showing the progressive opacification of iliac lymphatics (*arrowhead*) and iliac nodes (*double arrowheads*). (Kindly provided by Dr. Ruehm)

formance of indirect MR lymphography following the injection of a conventional extracellular contrast agent was assessed in rabbits [20, 21]. A total volume of 0.5 ml of gadoterate dimeglumine (Dotarem, Guerbet, Aulnay Sous Bois, France) was injected subcutaneously into the hind legs of 12 rabbits, resulting in the enhancement of four successive lymph node groups on T1-weighted images within 15–30 min. Similar results were also reported by the same authors in five human volunteers [22]. Figures 4 and 5 show examples of lymph duct

enhancement following the interstitial injection of an extracellular contrast agent. One of the drawbacks of using conventional extracellular gadolinium chelates is that much of the contrast agent is taken up by the venous system, with rapid enhancement of the bladder on T1-weighted images and rapid clearance from the regional nodes in contrast to macromolecular polymeric T1-type contrast agents.

Imaging lymph nodes

Although conventional lymphography has long been considered the "gold standard" for metastatic node identification, especially in lymphoma [23], its role is now limited owing to the development of the sentinel node procedure and of new emerging techniques in the field of MR imaging, ultrasound, and nuclear medicine (Table 2).

Unenhanced cross-sectional imaging of the lymphatic system

As shown, the anatomy of lymph nodes is complex. It is still unclear how cancer cells reach and enter the lymph nodes. Micrometastases involving axillary nodes in breast cancer are commonly reported in normal-sized nodes [24]. Because the gross anatomy of such invaded nodes remains unchanged, an intensive pathological search for suspicious nodes is mandatory, especially during sentinel node procedures [25]. The fact that contrast agents taken up by the lymphatic system are preferentially located in the peripherally located cortical areas of lymph nodes further suggests that the distinction of the sinus and the cortex of all lymph nodes on imaging is important [13]. Assessment of lymph nodes on high-resolution CT could provide useful morphological information. Uematsu et al. in a study of 212 axillary nodes demonstrated that helical CT could discriminate benign from malignant nodes using not only size criteria but also by identifying abnormal irregular-shaped eccentric cortexes [26]. The same applies to MR imaging. Regarding the study of axillary nodes in breast cancer on MR images, the visualization of the axilla with a conventional double breast coil can be achieved [27], but at the usual expense of nonuniform images [28]. Recent studies have thus demonstrated the importance of using dedicated surface coils when studying the axilla [29]. Although further studies are mandatory in order to assess the impact of these high-resolution studies, it is clear that noncontrast-enhanced imaging of lymph nodes could yield higher specificity figures on both CT and MR images if higher spatial resolution is systematically applied to nodal analysis.

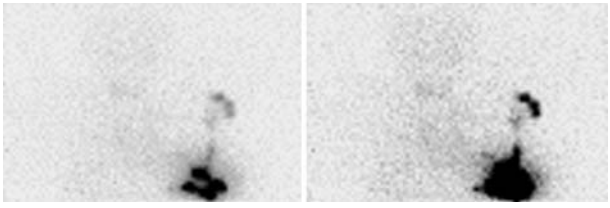

Fig. 6 Sentinel node identification in a 59-year-old patient with malignant melanoma at the left pectoral level 15 min after the intradermal injection of 29 Mbq of Tc99m nanocolloids at four locations around the tumor site. A group of three axillary lymph nodes are depicted. (Kindly provided by Dr. Emmanuel Itti)

Indirect lymphangioscintigraphy and sentinel node imaging

It is now well established for both melanoma [30] and breast cancer [31] that it is possible to identify the lymph nodes or sentinel nodes most likely to receive drainage from the primary tumor. This technique termed sentinel node imaging (SN) has gained increasing interest over the past few years as it could help avoid unnecessary invasive lymph node dissection procedures. The rationale for SN identification is twofold: first, early metastases occur in the first node, or sentinel node, which receives lymphatic drainage from the tumor; second, skip metastases during lymph node extension are rare. Thus, identification and removal of this sentinel node by means of limited surgical dissection could be sufficient for tumor staging. Based on several reports, the success rate of SN resection exceeds 90% and the overall accuracy exceeds 95% [32]. An example of SN identification is shown in Fig. 6.

Indirect interstitial CT and MR lymphography

Wisner et al. extensively studied the indirect opacification of regional lymph nodes following the injection of iodinated nanoparticles in animals [33]. Whether injected sub-cutaneously along podal extremities, or within the gastric and oral sub-mucosa, regional enhancement of lymph nodes was reported using CT, with a maximum occurring 24 h after injection. One of the main advantages of such a procedure would be to allow the study of specific nodes usually not well depicted on conventional CT. However, these preliminary studies have not yet been applied to humans, and both delivery techniques dose, and site of injection of the contrast agent, remain questioned. It has been demonstrated that smaller particles usually achieve earlier and increased nodal enhancement [34]. As mentioned previously, similar findings have been reported on MR following the interstitial injection of gadolinium chelates [18] resulting in sub-diaphragmatic nodal enhancement in animals and humans. Figure 5 shows an example of iliac node

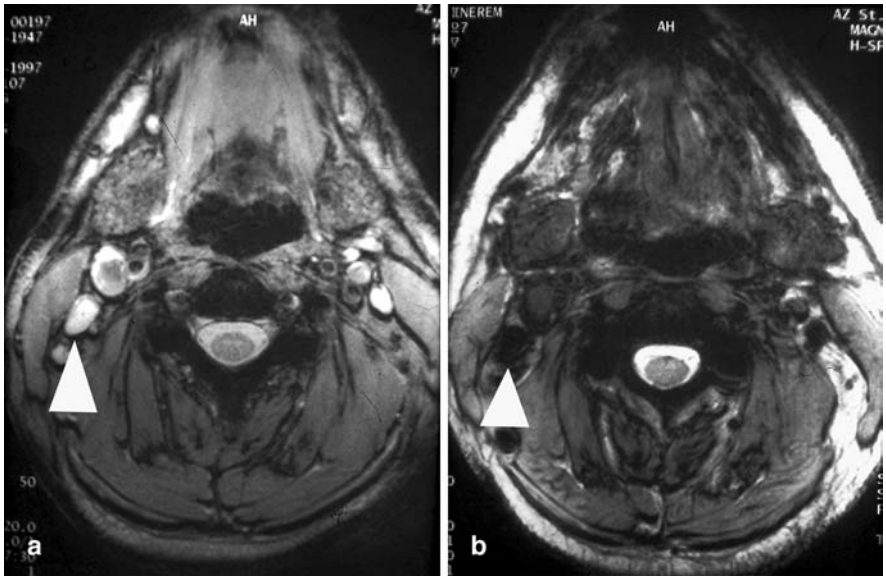

Fig. 7a, b MR staging in a 50-year-old patient with T2N1 clinical stage head and neck cancer. Transverse T2-weighted imaging at the submandibular level showing a 1.5-cm large ovoid mass (*arrowhead*) adjacent to the sternocleidomastoidal muscle with a high signal intensity on precontrast images **a** and showing homogeneous contrast enhancement and signal loss following the injection of the USPIO AMI-227 contrast agent (Sinerem) **b**, suggesting the diagnosis of inflammatory node without metastatic involvement

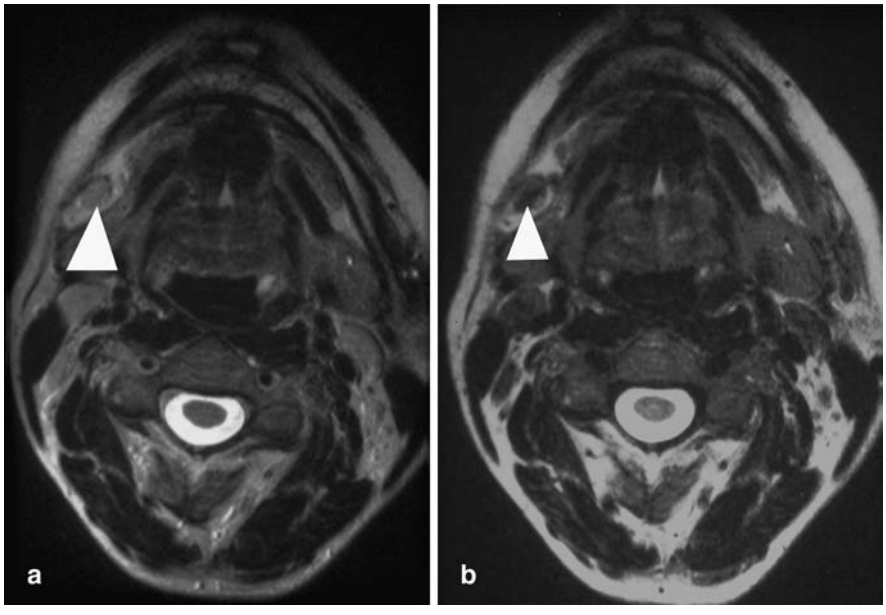

Fig. 8a, b MR staging in a 56-year-old patient with T3N0 clinical stage head and neck cancer. Transverse T2-weighted imaging at the submandibular level showing a small 1-cm lymph node (*arrowhead*) with homogeneous isosignal intensity on precontrast images **a** and heterogeneous enhancement after injection of AMI-227 contrast agent (Sinerem) **b**, suggesting the presence of metastatic involvement. Lymph node involvement was confirmed at surgery

enhancement following the interstitial injection of an extracellular Gd-Chelate contrast agent in a healthy volunteer.

USPIO enhanced MR lymphography

The intravenous infusion of USPIO agents such as Sinerem (AMI 227, Guerbet, Aulnay Sous Bois, France) at a mean dose of 30 μmol Fe/kg BW or 2.6 mg Fe/kg BW is followed by normal lymph node uptake resulting in a signal loss depicted 24 h after injection on T1- and especially on T2-weighted images because of magnetic susceptibility effects. It is thus possible to distinguish reactive from tumor-bearing nodes regardless of size criteria [14]. Tumor-involved nodes lack normal reticuloendothelial system cells which are replaced by metastatic cells. As a result, metastatic nodes do not take up the USPIO, and they lack signal loss. USPIOs thus behave as “negative” contrast agents. An example of normal-appearing and metastatic nodes following USPIO injection is shown in Figs. 7 and 8. The tolerance of Sinerem appeared satisfactory in a preliminary study of 30 patients [35]. Severe reactions were reported in only two patients, and the main discomfort reported was transient lumbar pain. In their study, Bellin et al. reported signal

intensity decrease in 76% of normal nodes with no significant signal intensity decrease in any metastatic nodes [35]. The lack of signal loss in 24% of normal nodes could be related to low doses of iron injection. The clinical applications of USPIO-enhanced lymphography are numerous. In a recent extensive review of the use of USPIO in 81 patients with head and neck cancer, Sigal et al. reported an 88% sensitivity and 77% specificity of USPIO-enhanced lymphography [36]. However, the positive predictive value (PPV) of Sinerem in this setting remained low, around 51%. The sensitivity rates, specificity rates, PPV, and NPV of USPIO-enhanced MR imaging of lymph nodes are highly variable apparently related to the evaluated anatomic region and the MR imaging technique. Thus, sensitivity figures above 90% were reported in a recent study of occult lymph node metastases in prostate cancer [37]. Similar results were also reported in the axillary evaluation of patients with breast cancer. Michel et al. in a recent axillary study of 20 patients with proven breast cancer reported an 82% sensitivity, 100% specificity, and 100% PPV of USPIO in the detection of metastatic nodes [38]. On a node-to-node basis, the respective sensitivity and specificity rates were 83 and 96%. In this study, heterogeneous uptake of USPIO or lack of uptake was considered indicative of malignant nodes. Similar criteria have been applied to pelvic gynecologic malignancies with similar sensitivity and specificity figures [39]. The impact of USPIO-enhanced lymphography in pelvic malignancies is of great concern since PET of this region could have a low sensitivity rate because of the systematic superimposition of the bladder [40].

Optimization of both the dose of contrast agent used and the MR technique are still necessary. Moreover, identification of micrometastases remains a challenge even with USPIO-enhanced lymphography and will probably gain more clinical impact with further improvements of high-resolution MR imaging techniques, especially on 3-T machines.

Positron emission tomography

FDG-PET, based on the increased uptake of deoxyglucose in metabolically active cells, has recently improved lymph node staging for many malignancies such as lymphomas [41, 42], breast cancer [43, 44], gynecologic malignancies [40, 45], or lung cancer [46], with sensitivity and specificity figures for correct nodal staging ranging close to 90%. New probes, such as C11-Choline, could also improve the detection of lymph node metastases that remain insensitive to FDG, for example, in prostate cancer [47]. Fusion techniques, including combined PET-CT, could also integrate the high anatomical resolution provided by CT and the high specificity and sensitivity provided by PET.

Role of ultrasound in lymph node assessment

The use of ultrasound (US) in the assessment of lymph nodes is well known [48]. Usual features of metastatic nodes include large size (more than 3 cm in melanoma, for example), round shape, loss of central hilus, intense hypoechogenicity, and presence of irregular lymph node edges [49]. A recent review highlighted the impact of power Doppler and color Doppler in the differential diagnosis of lymph node lesions [50]. Benign nodes, whether normal or reactive, could display a hilar type of vascular flow with simple or multiple central vessels within the nodes, as opposed to the peripheral vascular flow pattern more frequently encountered in metastatic nodes where vascular signals are distributed at the periphery of the nodes. Accuracy and specificity figures reported could reach 88 and 86%, respectively. However, one of the main drawbacks of US remains: nodes located deeply could remain inaccessible to conventional US as opposed to MR imaging or indirect CT lymphography. This limitation could be overcome with the use of contrast-enhanced US, which allows better depiction of the vascular flow and especially of the accessory peripheral vessels more frequently encountered in metastatic nodes [51–53]. Contrast-enhanced US lymphography, a new application of US contrast media with interstitially administered microbubbles, could even challenge SN detection methods, as shown very recently with the enhancement of close to 94% of sentinel nodes following the interstitial infusion of submicron-diameter bubbles in the hind legs of 11 dogs [54].

Conclusion

A better knowledge of both the anatomy and the physiology of the lymphatic system allows a better understanding of the rationale of lymphatic imaging. Recent advances in the fields of contrast agents, MR and CT devices, and nuclear medicine have demonstrated that lymphatic imaging no longer relies solely on conventional lymphography. Lymphatic vessels and lymph flow disorders can be studied with indirect MR lymphography following the interstitial injection of gadolinium chelates, while lymph nodes can be studied with indirect MR lymphography, USPIO-enhanced MR lymphography, contrast-enhanced ultrasound, or PET. The respective role of each imaging technique remains to be determined; however, the impact of nodal imaging could limit the rate of invasive diagnostic staging procedures for neoplasms with lymphatic extension.

References

1. Witte CL, Witte MH, Unger EC et al (2000) Advances in imaging of lymph flow disorders. Radiographics 20:1697–1719
2. Picard J-D (1995) Lymphatic circulation. S.I.A., Lavaur, France
3. Merrigan BA, Winter DC, O'Sullivan GC (1997) Chylothorax. Br J Surg 84:15–20
4. Moghimi SM, Bonnemain B (1999) Subcutaneous and intravenous delivery of diagnostic agents to the lymphatic system: applications in lymphoscintigraphy and indirect lymphography. Adv Drug Deliv Rev 37:295–312
5. Weissleder H, Weissleder R (1988) Lymphedema: evaluation of qualitative and quantitative lymphoscintigraphy in 238 patients. Radiology 167:729–735
6. Witte CL, Witte MH (1999) Diagnostic and interventional imaging of lymphatic disorders. Int Angiol 18:25–30
7. Weissleder R, Elizondo G, Josephson L et al (1989) Experimental lymph node metastases: enhanced detection with MR lymphography. Radiology 171:835–839
8. Weissleder R, Elizondo G, Wittenberg J, Rabito CA, Bengele HH, Josephson L (1990) Ultrasmall superparamagnetic iron oxide: characterization of a new class of contrast agents for MR imaging. Radiology 175:489–493
9. Jung CW (1995) Surface properties of superparamagnetic iron oxide MR contrast agents: ferumoxides, ferumoxtran, ferumoxsil. Magn Reson Imaging 13:675–691
10. Jung CW, Jacobs P (1995) Physical and chemical properties of superparamagnetic iron oxide MR contrast agents: ferumoxides, ferumoxtran, ferumoxsil. Magn Reson Imaging 13:661–674
11. Weissleder R, Elizondo G, Wittenberg J, Lee AS, Josephson L, Brady TJ (1990) Ultrasmall superparamagnetic iron oxide: an intravenous contrast agent for assessing lymph nodes with MR imaging. Radiology 175:494–498
12. Clement O, Rety F, Cuenod CA et al (1998) MR lymphography: evidence of extravasation of superparamagnetic nanoparticles into the lymph. Acad Radiol 5:S170–S172 (discussion S183–S174)
13. Rety F, Clement O, Siauve N et al (2000) MR lymphography using iron oxide nanoparticles in rats: pharmacokinetics in the lymphatic system after intravenous injection. J Magn Reson Imaging 12:734–739
14. Vassallo P, Matei C, Heston WD, McLachlan SJ, Koutcher JA, Castellino RA (1994) AMI-227-enhanced MR lymphography: usefulness for differentiating reactive from tumor-bearing lymph nodes. Radiology 193:501–506
15. Guimaraes R, Clement O, Bittoun J, Carnot F, Frija G (1994) MR lymphography with superparamagnetic iron nanoparticles in rats: pathologic basis for contrast enhancement. Am J Roentgenol 162:201–207
16. Hayashi S, Miyazaki M (1999) Thoracic duct: visualization at nonenhanced MR lymphography—initial experience. Radiology 212:598–600
17. Harika L, Weissleder R, Poss K, Zimmer C, Papisov MI, Brady TJ (1995) MR lymphography with a lymphotropic T1-type MR contrast agent: Gd-DTPA-PGM. Magn Reson Med 33:88–92
18. Staatz G, Nolte-Ernsting CC, Adam GB et al (2001) Interstitial T1-weighted MR lymphography: lipophilic perfluorinated gadolinium chelates in pigs. Radiology 220:129–134
19. Misselwitz B, Schmitt-Willich H, Michaelis M, Oellinger JJ (2002) Interstitial magnetic resonance lymphography using a polymeric t1 contrast agent: initial experience with Gadomer-17. Invest Radiol 37:146–151
20. Ruehm SG, Corot C, Debatin JF (2001) Interstitial MR lymphography with a conventional extracellular gadolinium-based agent: assessment in rabbits. Radiology 218:664–669
21. Bellin MF, Vasile M, Morel-Precetti S (2003) Currently used non-specific extracellular MR contrast media. Eur Radiol 12:2688–2698
22. Ruehm SG, Schroeder T, Debatin JF (2001) Interstitial MR lymphography with gadoterate meglumine: initial experience in humans. Radiology 220:816–821
23. Moskovic E, Fernando I, Blake P, Parsons C (1991) Lymphography—current role in oncology. Br J Radiol 64:422–427
24. Cserni G (1999) Metastases in axillary sentinel lymph nodes in breast cancer as detected by intensive histopathological work up. J Clin Pathol 52:922–924
25. Dowlatshahi K, Fan M, Snider HC, HabibFA (1997) Lymph node micrometastases from breast carcinoma: reviewing the dilemma. Cancer 80:1188–1197
26. Uematsu T, Sano M, Homma K (2001) In vitro high-resolution helical CT of small axillary lymph nodes in patients with breast cancer: correlation of CT and histology. Am J Roentgenol 176:1069–1074
27. Mumtaz H, Hall-Craggs MA, Davidson T et al (1997) Staging of symptomatic primary breast cancer with MR imaging. Am J Roentgenol 169:417–424
28. Konyer NB, Ramsay EA, Bronskill MJ, Plewes DB (2002) Comparison of MR imaging breast coils. Radiology 222:830–834
29. Luciani A, Dao TH, Lapeyre M et al (2004) Simultaneous bilateral breast and high-resolution axillary MRI of patients with breast cancer: preliminary results. Am J Roentgenol (in press)
30. Morton DL, Wen DR, Wong JH et al (1992) Technical details of intraoperative lymphatic mapping for early stage melanoma. Arch Surg 127:392–399
31. Krag DN (1999) The sentinel node for staging breast cancer: current review. Breast Cancer 6:233–236
32. Whitworth P, McMasters KM, Tafra L, Edwards MJ (2000) State-of-the-art lymph node staging for breast cancer in the year 2000. Am J Surg 180:262–267
33. Wisner ER, Katzberg RW, Koblik PD et al (1995) Indirect computed tomography lymphography of subdiaphragmatic lymph nodes using iodinated nanoparticles in normal dogs. Acad Radiol 2:405–412
34. McIntire GL, Bacon ER, Illig KJ et al (2000) Time course of nodal enhancement with CT X-ray nanoparticle contrast agents: effect of particle size and chemical structure. Invest Radiol 35:91–96
35. Bellin MF, Roy C, Kinkel K et al (1998) Lymph node metastases: safety and effectiveness of MR imaging with ultrasmall superparamagnetic iron oxide particles—initial clinical experience. Radiology 207:799–808
36. Sigal R, Vogl T, Casselman J et al (2002) Lymph node metastases from head and neck squamous cell carcinoma: MR imaging with ultrasmall superparamagnetic iron oxide particles (Sinerem MR)—results of a phase-III multicenter clinical trial. Eur Radiol 12:1104–1113
37. Harisinghani MG, Barentsz J, Hahn PF et al (2003) Noninvasive detection of clinically occult lymph-node metastases in prostate cancer. N Engl J Med 348:2491–2499
38. Michel SC, Keller TM, Frohlich JM et al (2002) Preoperative breast cancer staging: MR imaging of the axilla with ultrasmall superparamagnetic iron oxide enhancement. Radiology 225:527–536

39. Harisinghani MG, Saini S, Slater GJ, Schnall MD, Rifkin MD (1997) MR imaging of pelvic lymph nodes in primary pelvic carcinoma with ultrasmall superparamagnetic iron oxide (Combidex): preliminary observations. J Magn Reson Imaging 7:161–163
40. Williams AD, Cousins C, Soutter WP et al (2001) Detection of pelvic lymph node metastases in gynecologic malignancy: a comparison of CT, MR imaging, and positron emission tomography. Am J Roentgenol 177:343–348
41. Hong SP, Hahn JS, Lee JD, Bae SW, Youn MJ (2003) 18F-Fluorodeoxyglucose-positron emission tomography in the staging of malignant lymphoma compared with CT and 67 Ga Scan. Yonsei Med J 44:779–786
42. Friedberg JW, Chengazi V (2003) PET scans in the staging of lymphoma: current status. Oncologist 8:438–447
43. Barranger E, Grahek D, Antoine M, Montravers F, Talbot JN, Uzan S (2003) Evaluation of fluorodeoxyglucose positron emission tomography in the detection of axillary lymph node metastases in patients with early-stage breast cancer. Ann Surg Oncol 10:622–627
44. Eubank WB, Mankoff DA, Takasugi J et al (2001) 18fluorodeoxyglucose positron emission tomography to detect mediastinal or internal mammary metastases in breast cancer. J Clin Oncol 19:3516–3523
45. Lin WC, Hung YC, Yeh LS, Kao CH, Yen RF, Shen YY (2003) Usefulness of (18)F-fluorodeoxyglucose positron emission tomography to detect paraaortic lymph nodal metastasis in advanced cervical cancer with negative computed tomography findings. Gynecol Oncol 89:73–76
46. Antoch G, Stattaus J, Nemat AT et al (2003) Non-small cell lung cancer: dual-modality PET/CT in preoperative staging. Radiology 229:526–533
47. Picchio M, Messa C, Landoni C et al (2003) Value of [11C]choline-positron emission tomography for re-staging prostate cancer: a comparison with [18F]fluorodeoxyglucose-positron emission tomography. J Urol 169:1337–1340
48. Vassallo P, Wernecke K, Roos N, Peters PE (1992) Differentiation of benign from malignant superficial lymphadenopathy: the role of high-resolution US. Radiology 183:215–220
49. Tregnaghi A, De Candia A, Calderone M et al (1997) Ultrasonographic evaluation of superficial lymph node metastases in melanoma. Eur J Radiol 24:216–221
50. Steinkamp HJ, Wissgott C, Rademaker J, Felix R (2002) Current status of power Doppler and color Doppler sonography in the differential diagnosis of lymph node lesions. Eur Radiol 12:1785–1793
51. Moritz JD, Ludwig A, Oestmann JW (2000) Contrast-enhanced color Doppler sonography for evaluation of enlarged cervical lymph nodes in head and neck tumors. Am J Roentgenol 174:1279–1284
52. Yang WT, Metreweli C, Lam PK, Chang J (2001) Benign and malignant breast masses and axillary nodes: evaluation with echo-enhanced color power Doppler US. Radiology 220:795–802
53. Schmid-Wendtner MH, Partscht K, Korting HC, Volkenandt M (2002) Improved differentiation of benign and malignant lymphadenopathy in patients with cutaneous melanoma by contrast-enhanced color Doppler sonography. Arch Dermatol 138:491–497
54. Wisner ER, Ferrara KW, Short RE, Ottoboni TB, Gabe JD, Patel D (2003) Sentinel node detection using contrast-enhanced power Doppler ultrasound lymphography. Invest Radiol 38:358–365